

# Generalized Parton Distributions in Deeply Virtual Lepton Scattering Processes

---

**Gary Goldstein\***

*Tufts University*

*E-mail:* [gary.goldstein@tufts.edu](mailto:gary.goldstein@tufts.edu)

**S. Liuti**

*University of Virginia*

*E-mail:* [s14y@virginia.edu](mailto:s14y@virginia.edu)

Spin and transverse momentum dependent Generalized Parton Distributions (GPDs) exist at the interface between the non-perturbative regime of QCD hadron structure and observable quantities. The distributions appear as linear superpositions and convolutions within helicity amplitudes for parton-nucleon scattering processes, which, in turn, occur in amplitudes for leptonproduction processes. We have developed a “flexible model” of quark and gluon GPDs that incorporates diquark and other spectators, Regge behavior and evolution. Chiral even GPDs determine deeply virtual Compton scattering amplitudes and are compared with cross section and polarization data. The chiral odd GPDs can be generated from these via parity relations. Those chiral odd GPDs, including “transversity”, lead to predictions for pseudoscalar leptonproduction. We will present relations between crucial quark-nucleon or gluon-nucleon GPDs and the rich array of angular distributions in Deeply Virtual Scattering processes.

*QCD Evolution 2016*

*May 30-June 03, 2016*

*National Institute for Subatomic Physics (Nikhef) in Amsterdam*

---

\*Speaker.

## 1. Introduction

The spin of the hadrons depends on the distributions of spin and orbital angular momenta (OAM) of the fundamental constituents, quarks and gluons. The quark and gluon field correlations in the nucleon are indirectly measurable through electroproduction processes. The angular momenta associated with the quark and gluon fields within QCD, are encoded in the transverse momentum distributions (TMDs) [1], the Generalized Parton Distributions (GPDs) [2] and the even more "General" TMDs (GTMDs) [3]. We developed an extensive spectator model for the valence quark chiral even and chiral odd GPDs that we will summarize. We have begun to extend the spectator model of the GPDs to include sea quark and gluon distributions. When assembled together and Fourier Transformed, these can provide a 3-dimensional picture of the angular momentum structure of the nucleon.

Initial work [4] in constructing a spectator model for the chiral even GPDs,  $H^q(X, \zeta, t)$  and  $E_q(X, \zeta, t)$ , showed considerable promise in incorporating constraints and in confronting data. This approach was extended to include all four of the chiral even valence quark GPDs, in conjunction with Deeply Virtual Compton Scattering (DVCS), in a series of papers that developed the "flexible model", which is a "Reggeized diquark model" ( $\mathbf{RxDq}$ ) [5, 6].

Of particular interest among spin dependent pdf's were the nucleon's *transversity* structure functions, e.g.  $h_1(x)$  - the probability of finding a definite transversity quark inside a transversely polarized nucleon. These distributions are chiral odd, and can be observed indirectly in Semi-Inclusive Deep Inelastic Scattering (SIDIS), where they are convoluted with fragmentation functions, or in the Drell-Yan process in conjunction with another chiral-odd partner. We realized that they also contribute to exclusive electroproduction processes, particularly Deeply Virtual Meson Production (DVMP), for pseudoscalar mesons through leading twist chiral odd GPDs. These enter at next order in DVMP for the factorized meson distribution function - twist 3. The *transversity* GPDs  $H_T^q(x, \xi, t)$  have the limiting form  $H_T^q(x, 0, 0) = h_1^q(x)$ , hence, from the DVMP processes, transversity can be determined. This had been one focus of the model in the past. However, to begin to parameterize the chiral odd GPDs, the more far-reaching chiral even GPDs were modeled. Subsequently, noting that the gluon GPDs can have a major role in processes measurable at lepton accelerators, the LHC and at a future Electron-Ion-Collider we have begun to extend the spectator model. We will present some preliminary developments for those GPDs. Novel measurements that relate to GTMDs will be mentioned also.

## 2. Formalism

It is useful for later applications to begin the formalism for GPDs with the more generalized objects, the quark GTMDs [3]. Then the form of quark distributions in the nucleon is given by off-diagonal matrix elements of bilocal field operators,

$$W_{\Lambda\Lambda'}^{[\Gamma]}(\bar{P}, x, \vec{k}_T, \Delta, N; \eta) = \frac{1}{2} \int dk^- \frac{d^4z}{(2\pi)^4} e^{ikz} \langle P', \Lambda' | \bar{\psi}\left(-\frac{z}{2}\right) \Gamma \mathscr{W}\left(-\frac{z}{2}, \frac{z}{2} | n\right) \psi\left(\frac{z}{2}\right) | P, \Lambda \rangle \quad (2.1)$$

with  $\Gamma$  a Dirac matrix,  $\mathscr{W}$  the appropriate gauge link,  $\bar{P} = (P + P')/2$ ,  $\Delta = P' - P$  and  $N = M^2 n / \bar{P} \cdot n$ , with  $n$  the usual light-like vector, and  $\eta = \text{sign}(n_0)$  (see [3] for details). The integration over  $k^-$

places the matrix element at  $z^+ = 0$  on the light cone. These GTMDs have both the nucleon momentum transfer  $\Delta$  and the outgoing parton momentum  $k$  as variables. As such, they are “unintegrated” parton distributions. Geometrically, the orientation of the partons requires the specification of two planes: the  $k_T$  plane formed by  $\vec{k}_T, \vec{P}_3$ ; the  $\Delta$  plane formed by the  $\vec{\Delta}_T, \vec{P}_3$ .

The TMDs are obtained by setting  $\Delta = 0$  in Eq. 2.1,

$$\Phi_{\Lambda\Lambda'}^{[\Gamma]}(\vec{P}, x, \vec{k}_T, N; \eta) = W_{\Lambda\Lambda'}^{[\Gamma]}(\vec{P}, x, \vec{k}_T, \Delta = 0, N; \eta), \quad (2.2)$$

so that this becomes a distribution and the  $k_T$  with the  $\vec{P}_3$  defines a single plane. This  $k_T$  plane will be distinct from the lepton plane, as will be seen in the TMD-based SIDIS process  $l + N \rightarrow l' + \gamma$  or hadron +  $X$ , the planes being related by an azimuthal angle,  $\phi$ .

The GPDs are obtained from Eq. 2.1 by integrating over all  $k$ , leaving  $\Delta$  a kinematic variable and forming the  $\Delta$  kinematic plane with,

$$\begin{aligned} F_{\Lambda'\Lambda}^{[\Gamma]}(\vec{P}, x, \Delta, N) &= \int d^2\vec{k}_T W_{\Lambda\Lambda'}^{[\Gamma]}(\vec{P}, x, \vec{k}_T, \Delta, N; \eta) \\ &= \frac{1}{2} \int \frac{dz^-}{2\pi} e^{ix\bar{P}^+z^-} \langle P', \Lambda' | \bar{\psi}\left(-\frac{z}{2}\right) \Gamma \psi\left(\frac{z}{2}\right) | P, \Lambda \rangle \Big|_{z^+=0, \vec{z}_T=0}, \end{aligned} \quad (2.3)$$

These quark GPDs are defined (at leading twist) as the matrix elements of the projections of the unintegrated quark-quark proton correlator (see Ref.[7] for a detailed overview), where  $\Gamma = \gamma^+, \gamma^+ \gamma_5, i\sigma^{i+} \gamma_5 (i = 1, 2)$  for leading twist, and the target’s spins are  $\Lambda, \Lambda'$ . These are amplitudes rather than distributions, and appear in bilinear form for exclusive processes. The spin structures of GPDs that are directly related to spin dependent observables are most effectively expressed in term of helicity dependent amplitudes, developed extensively for the covariant description of two body scattering processes (see also Ref.[7]). For the GPDs, decomposing the quark fields into definite helicities,  $\lambda, \lambda'$ , produces a form analogous to 2-body quark-nucleon helicity amplitudes,  $A_{\Lambda'\lambda', \Lambda\lambda}(X, \zeta, t)$  [7].

There are four chiral-even, helicity conserving quark GPDs,  $H, E, \tilde{H}, \tilde{E}$  [8] and four additional chiral-odd GPDs, at leading twist 2, that flip quark helicity by one unit,  $H_T, E_T, \tilde{H}_T, \tilde{E}_T$  [7, 9]. There are two questions to address: How to model the 8 GPDs? How to measure them? We have done extensive work on answering these questions [5, 6, 10, 11].

At this point the discussion has been aimed at the quark distributions. On the same level - at leading “twist” - and of growing importance are the *gluon distributions*. The helicity conserving gluon GPDs with t-channel even parity are defined analogously to quark and/or antiquark correlators:

$$\begin{aligned} F^g &= \frac{1}{\bar{P}^+} \int \frac{dz^-}{2\pi} e^{ix\bar{P}^+z^-} \langle P', \Lambda' | G^{+\mu} \left(-\frac{1}{2}z\right) G_{\mu}^+ \left(\frac{1}{2}z\right) | P, \Lambda \rangle \Big|_{z^+=0, \vec{z}_T=0} \rightarrow \\ &= \frac{1}{\bar{P}^+} \int \frac{dz^-}{2\pi} e^{ix\bar{P}^+z^-} \langle P', \Lambda' | G^{+j} \left(-\frac{1}{2}z\right) G^j \left(\frac{1}{2}z\right) | P, \Lambda \rangle \Big|_{z^+=0, \vec{z}_T=0} = \\ &= \frac{1}{2\bar{P}^+} \bar{U}(P', \Lambda') [H^g(x, \xi, t) \gamma^+ + E^g(x, \xi, t) \frac{i\sigma^{+\alpha}(-\Delta_\alpha)}{2M}] U(P, \Lambda) \end{aligned} \quad (2.4)$$

and for t-channel odd parity

$$\tilde{F}^g = \frac{-i}{\bar{P}^+} \int \frac{dz^-}{2\pi} e^{ix\bar{P}^+z^-} \langle P', \Lambda' | G^{+\mu} \left(-\frac{1}{2}z\right) \tilde{G}_{\mu}^+ \left(\frac{1}{2}z\right) | P, \Lambda \rangle \Big|_{z^+=0, \vec{z}_T=0} \rightarrow$$

$$\begin{aligned} & \frac{-i}{\bar{P}^+} \int \frac{dz^-}{2\pi} e^{ix\bar{P}^+z^-} \langle P', \Lambda' | G^{+j}(-\frac{1}{2}z) \tilde{G}^{+j}(\frac{1}{2}z) | P, \Lambda \rangle \Big|_{z^+=0, \vec{z}_T=0} = \\ & \frac{1}{2\bar{P}^+} \bar{U}(P', \Lambda') [\tilde{H}^g(x, \xi, t) \gamma^+ \gamma_5 + E^g(x, \xi, t) \frac{\gamma_5(-\Delta^+)}{2M}] U(P, \Lambda), \end{aligned} \quad (2.5)$$

summing over transverse indices  $j = 1, 2$ , and using the dual gluon field strength

$$\tilde{G}^{\mu\nu}(x) = \frac{1}{2} \varepsilon^{\mu\nu\alpha\beta} G_{\alpha\beta}(x).^1$$

The transverse polarization components enter here because we take leading twist 2 and the ‘‘good’’ components of the gluon polarization 4-vectors, which are transverse polarization (helicity  $\pm 1$ ) on-shell. The longitudinal polarization (helicity 0) enters at twist 3 (having one fewer transverse, good component of spin). There are also contributions involving the transverse helicity flip ( $\pm 1 \rightarrow \mp 1$ ), which can be thought of as gluon states of transversity, or equivalently, linear polarization states [12]. The gluon ‘‘transversity’’ distributions are defined as (Ref. [7])

$$\begin{aligned} F_T^g &= -\frac{1}{\bar{P}^+} \int \frac{dz^-}{2\pi} e^{ix\bar{P}^+z^-} \langle P', \Lambda' | \mathbf{S} G^{+j}(-\frac{1}{2}z) G^{+k}(\frac{1}{2}z) | P, \Lambda \rangle \Big|_{z^+=0, \vec{z}_T=0} \\ &= \mathbf{S} \frac{1}{2\bar{P}^+} \frac{\bar{P}^+ \Delta^j - \Delta^+ \bar{P}^j}{2M\bar{P}^+} \\ &\quad \times \bar{U}(P', \Lambda') \left[ H_T^g(x, \xi, t) i\sigma^{+k} + \tilde{H}_T^g \frac{\bar{P}^+ \Delta^k - \Delta^+ \bar{P}^k}{M^2} \right. \\ &\quad \left. + E_T^g(x, \xi, t) \frac{\gamma^+ \Delta^k - \Delta^+ \gamma^k}{2M} + \tilde{E}_T^g \frac{\gamma^+ \bar{P}^k - \bar{P}^+ \gamma^k}{M} \right] U(P, \Lambda) \end{aligned} \quad (2.6)$$

wherein  $\mathbf{S}$  symmetrizes in  $(j, k)$  and removes the trace. The modeling of these gluon transversity distributions will be considered in a forthcoming publication. It is interesting to note that such double flip gluon transitions can be accessed through double photon helicity flip in DVCS, for which the quarks will not contribute. Measurement of outgoing photon helicity, though, is not accessible. Alternatively, Deeply Virtual vector meson production and lepton pair production have been studied and will be developed further in the near future.

### 3. Flexible Model

The basis of our model of parton distributions is the connection to observables through the ‘‘handbag’’ approximation and evolution. The various distributions are then related to quark or gluon plus nucleon scattering-type amplitudes. We model these via nucleon transitions into quark (or antiquark or gluon) and a spectator (or light front wave functions or lowest Fock states). That is to say, the leading Fock state for the nucleon is assumed to be a quark (color 3) and diquark (color  $\bar{3}$ ) configuration, like the lowest two-body orbital angular momentum  $L = 0$  bound state, wherein the diquark can be a scalar of antisymmetric flavor or an axial vector of symmetric flavor. The quark-proton ‘‘scattering amplitudes’’ at leading order are convolutions of proton-quark-diquark vertices. The quark proton helicity amplitudes describe a two body process,  $q'(k')P \rightarrow X \rightarrow q(k)P'$ , where  $q(k)$  corresponds to the ‘‘struck quark’’. The intermediate diquark system,  $X$ , can have  $J^P = 0^+$

<sup>1</sup>With this convention  $H_g$  reduces to the pdf  $xg(x, 0, 0)$ .

(scalar), or  $J^P = 1^+$  (axial vector). The amplitudes for the Scalar diquark are (see [5, 10] for the full set of relations):

$$A_{\Lambda'\lambda',\Lambda\lambda}^{(0)} = \int d^2k_\perp \phi_{\Lambda'\lambda'}^*(k', P') \phi_{\Lambda\lambda}(k, P), \quad (3.1)$$

where  $\phi_{\Lambda\lambda}(k, P)$  is the nucleon-quark-scalar diquark vertex or light front wave function.

Next we consider ‘‘Reggeization’’, that is, we extend the diquark model formalism to low  $X$  by allowing the spectator system’s mass to vary up to very large values. This is accomplished by convoluting the GPD structures obtained in Eqs.(3.1) with a ‘‘spectral function’’,  $\rho(M_X^2)$ , where  $M_X^2$  is the spectator’s mass,

$$F_T^q(X, \zeta, t) = \mathcal{N}_q \int_0^\infty dM_X^2 \rho(M_X^2) F_T^{(m_q, M_X^q)}(X, \zeta, t; M_X) \approx R_{p_q}^{\alpha_q, \alpha'_q}(X, \zeta, t) G_{M_X, m}^{M_\Lambda}(X, \zeta, t) \quad (3.2)$$

with  $F_T^{(m_q, M_X^q)}(X, \zeta, t; M_X)$  any of the quark-diquark model GPDs for definite mass diquark. The spectral function was constructed in Refs.[5, 6] so that it approximately behaves as  $(M_X^2)^\alpha$  for  $M_X^2 \rightarrow \infty$  and  $\delta(M_X^2 - \bar{M}_X^2)$  for  $M_X^2$  at a few  $\text{GeV}^2$ , where  $0 < \alpha < 1$ , and  $\bar{M}_X$  is in the GeV range, with  $\alpha'_q(X) = \alpha'_q(1 - X)^{p_q}$ . The functions  $G_{M_X, m}^{M_\Lambda}$  and  $R_{p_q}^{\alpha_q, \alpha'_q}$  are the quark-diquark and Regge contributions, respectively. The chiral even quark GPDs integrate to the nucleon form factors, which constrains the GPD t-dependence,

$$\int_0^1 H^q(X, \zeta, t) = F_1^q(t), \int_0^1 E^q(X, \zeta, t) = F_2^q(t), \int_0^1 \tilde{H}^q(X, \zeta, t) = G_A^q(t), \int_0^1 \tilde{E}^q(X, \zeta, t) = G_P^q(t). \quad (3.3)$$

where  $F_1^q(t)$  and  $F_2^q(t)$  are the Dirac and Pauli form factors for the quark  $q$  components in the nucleon.  $G_A^q(t)$  and  $G_P^q(t)$  are the axial and pseudoscalar form factors. Furthermore,  $H(x, 0, 0) = f_1(x)$  and  $\tilde{H}(x, 0, 0) = g_1(x)$ . With these constraints, the quark GPDs that fit DVCS results [5] are

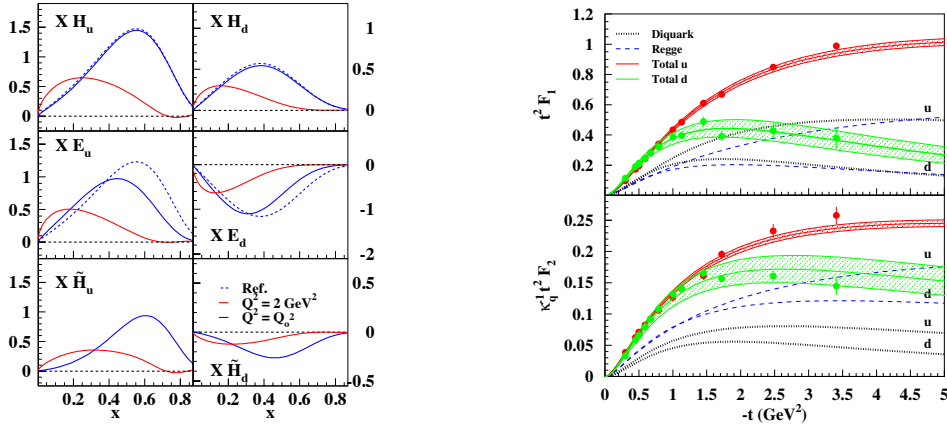


**Figure 1:** Left: Chiral even u and d-quark GPDs at the initial scale and  $Q^2 = 2\text{GeV}^2$  Adapted from Ref. [5]. Right: Contributions to EM Form Factors  $F_1(t)$ ,  $F_2(t)$  from best fit valence quark integrated GPDs. [6], [13]. Adapted from Ref. [6].

shown in Fig. 1 along with the improved constraints [6] determined by precision measurements

of the EM form factors [13]. The u and d GPDs are shown for two values of  $Q^2$ , obtained by application of the DGLAP evolution equations.

Our model for evaluating the chiral-odd GPDs extended the Reggeized diquark model for chiral-even GPDs, to the chiral-odd transversity sector, using parity relations for the vertices in Eq. 3.1. See Fig. 2 (Left) for all four of the predicted complex Compton Form Factors vs.  $t$  at one low  $Q^2$  value. The successful phenomenology for the chiral-odd GPDs applied to  $\pi^0$  electro-production is shown in several publications [10, 11] - experimental comparisons were presented in Refs. [14, 15], among others. An example of the  $t$ -dependence for one kinematic bin of  $x_{Bj}$  and  $Q^2$  is shown in Fig. 2 (Right), as we discuss below.

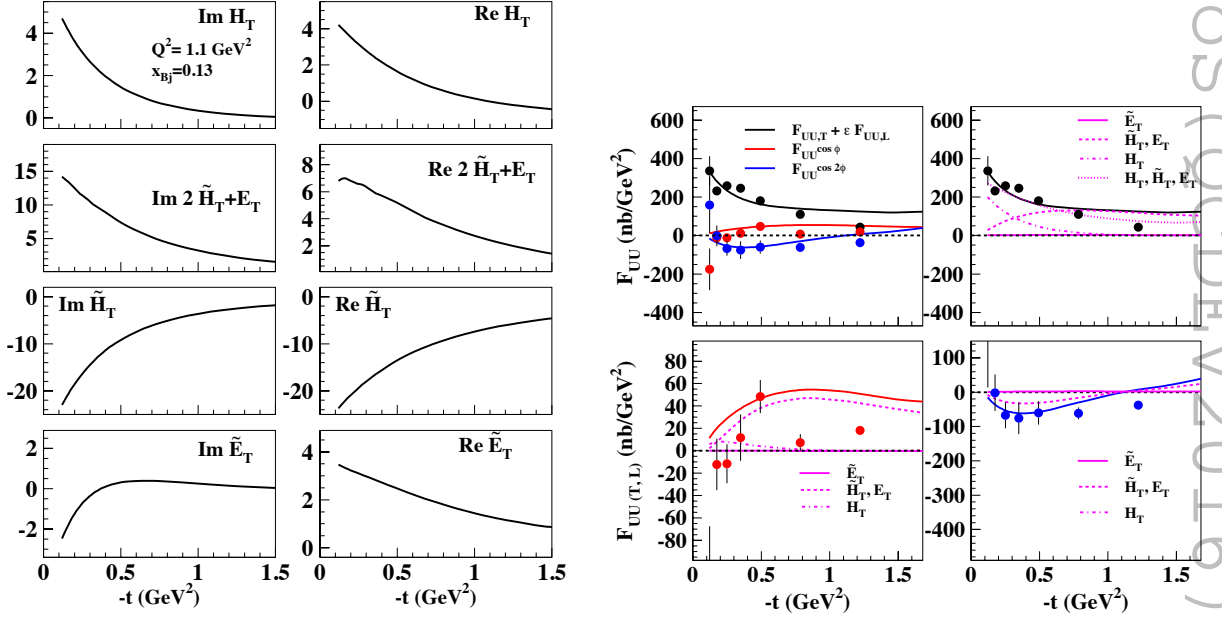


**Figure 2: Left:** Chiral Odd CFFs entering the process  $\gamma^* p \rightarrow \pi^0 p'$ . From top to bottom  $\Im \mathcal{H}_T$  (left),  $\Re \mathcal{H}_T$  (right);  $\Im [2\tilde{\mathcal{H}}_T + \mathcal{E}_T]$  (left),  $\Re [2\tilde{\mathcal{H}}_T + \mathcal{E}_T]$  (right);  $\Im \tilde{\mathcal{H}}_T$  (left),  $\Re \tilde{\mathcal{H}}_T$  (right);  $\Im \tilde{\mathcal{E}}_T$  (left),  $\Re \tilde{\mathcal{E}}_T$  (right). The various CFFs are plotted vs.  $-t$  for the kinematic bin  $x_{Bj} = 0.13$ ,  $Q^2 = 1.1$  GeV<sup>2</sup>. **Right:** Unpolarized cross section components,  $F_{UU,T} + \epsilon F_{UU,L}$ ,  $F_{UU}^{\cos \phi}$ , and  $F_{UU}^{\cos 2\phi}$  in the kinematical bin,  $x_{Bj} = 0.27$ ,  $Q^2 = 2.2$  GeV<sup>2</sup>. The upper left panel shows all components along with the data from Ref.[14]. The other panels show the contributions from the various GPDs to particular sub-cross sections. Adapted from Ref. [11].

For the gluon GPDs, the model is generalized from the spectator picture for quark GPDs [16]. The nucleon decomposes into a gluon and a color octet baryon, so that the overall color is a singlet. The color octet baryon contains components that have the same flavor as the nucleon, are Fermionic (with color $\otimes$ flavor $\otimes$ spin being antisymmetric under quark label exchanges), and include spin 1/2 and spin 3/2 flavor octets (belonging to the mixed symmetry 70-plet of flavor $\otimes$ spin SU(6)). We can select spin 1/2 for simplicity. This provides sufficient parameterization to fit the  $H_g(x, 0, 0)$  to the pdf  $g(x)$ . Evolving with  $Q^2$  also requires a sea quark  $\gamma$  contribution, which we take in an analogous spectator picture with  $N \rightarrow \bar{u} \oplus (uuud)$  or  $\bar{d} \oplus (uudd)$ . The constraints on the gluon distributions are the unpolarized gluon pdfs for  $H_g(X, 0, 0)$ . This is shown for one  $Q^2$  value in Fig. 3 (Left) for the complete set of partons: for the gluons, the valence and sea u-quarks at  $Q^2 = 5$ . The full DGLAP

evolution is applied to obtain the best parametrization. To extend the unpolarized gluon GPDs to non-zero  $t$ , constraining form factors would be useful. One available functional form is provided by QCD sum rules for gluons [18]. We show the  $t$ -dependence of our spectator model by itself, without Regge behavior incorporated, compared to the sum rules and pure Regge behavior (for small  $x$ ), in Fig. 3 (Right). This indicates that the spectator model already incorporates appropriately declining  $t$ -dependence. This can be seen in the (preliminary) Fig. 4.

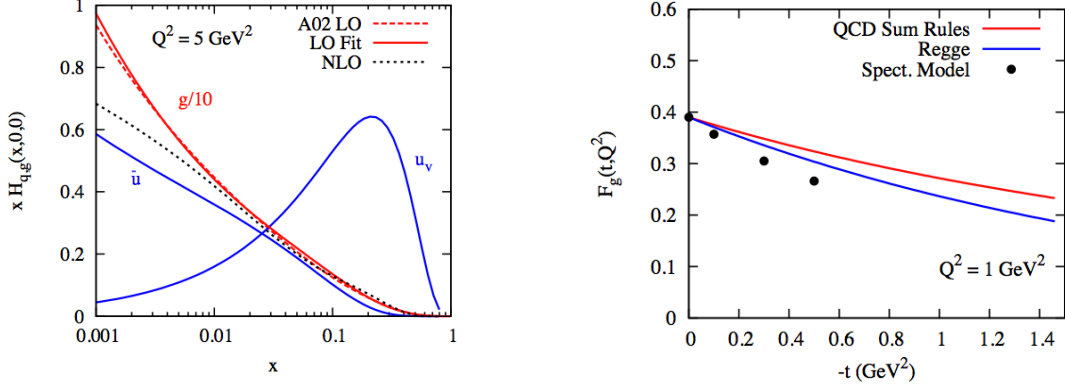


**Figure 3:** Left: Fits of unpolarized valence u-quark, sea u-quark and gluon form factor  $xH_g(x, 0, 0)$  as a function of  $x$  from spectator model [16], compared with Alekhin [17]. Right: Unpolarized gluon form factor  $F_g(t, Q^2)$  as a function of  $t$  from spectator model [16], compared with QCD Sum Rule [18] and Regge behavior.

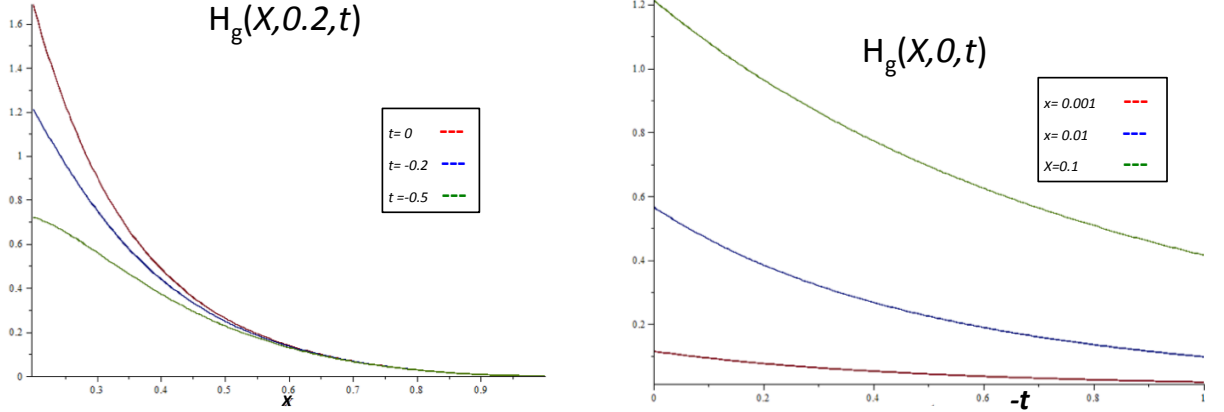


**Figure 4:** (color online) **Left:** Graphs of  $H_g(X, 0.2, t)$ , i.e.  $\zeta = 0.2$ , plotted against  $X$  for the initial scale of  $Q^2$  with three values of  $-t$ . Note that the graph is in the DGLAP region only. **Right:** Graphs of  $H_g(X, 0, t)$  plotted against  $-t$  for three values of  $X$  and the initial scale of  $Q^2$ . Courtesy J. Poage and adapted from Ref. [16].

#### 4. Observables and data

DVCS accesses Chiral Even GPDs through various cross sections and asymmetries. The GPDs, or their corresponding Compton Form Factors, enter as bilinears in pure DVCS or pure

Bethe-Heitler in these observables, or linearly via Bethe-Heitler  $\otimes$  DVCS interference. On the other hand, DV $\pi^0$ S accesses 2 Chiral Even + 4 Chiral Odd GPDs that enter bilinearly via  $d\sigma/d\Omega$  & polarization asymmetries. The result of experimental observations that  $d\sigma_T > d\sigma_L$  is that the chiral odd GPDs dominate, even though these GPDs enter the overall amplitudes through twist 3  $\pi^0$  distribution amplitudes.

In Ref.[10], after showing how DV $\pi^0$ P can be described in terms of chiral-odd GPDs, we estimated all of their contributions to the various observables with particular attention to the ones which were sensitive to the values of the tensor charge. The connection of the correlator, Eq.(2.3), with the helicity amplitudes for  $\pi^0$  electroproduction proceeds by introducing a factorized form [10, 11],

$$f_{\Lambda\gamma 0}^{\Lambda\Lambda'}(\zeta, t) = \sum_{\lambda, \lambda'} g_{\Lambda\gamma 0}^{\lambda\lambda'}(X, \zeta, t, Q^2) \otimes A_{\Lambda'\lambda'; \Lambda\lambda}(X, \zeta, t), \quad (4.1)$$

where the helicities of the virtual photon and the initial proton are,  $\Lambda_\gamma$ ,  $\Lambda$ , and the helicities of the produced pion and final proton are 0, and  $\Lambda'$ , respectively. This describes a factorization into a ‘‘hard part’’,  $g_{\Lambda\gamma 0}^{\lambda\lambda'}$  for the partonic subprocess  $\gamma^* + q \rightarrow \pi^0 + q$ , and a ‘‘soft part’’ given by the quark-proton helicity amplitudes,  $A_{\Lambda'\lambda'; \Lambda\lambda}$  that contain the GPDs. We assumed this can be factorized, within the assumptions of the model, which goes beyond the proven leading twist factorization with chiral even GPDs [19]. The expressions for the chiral-odd quark-nucleon helicity amplitudes in terms of GPDs [7] are of the form

$$A_{++,-} = \sqrt{1 - \xi^2} \left[ H_T + \frac{t_0 - t}{4M^2} \tilde{H}_T - \frac{\xi^2}{1 - \xi^2} E_T + \frac{\xi}{1 - \xi^2} \tilde{E}_T \right], \dots \quad (4.2)$$

where we use the symmetric notation for the kinematic variables. Analogous forms have been written for the chiral even and the remaining chiral odd sectors [7].

The fitting procedure of GPDs is quite complicated owing to its many different steps. We described the ‘‘recursive procedure’’ that we used for the chiral even GPDs, the flexible model, in Ref. [5]. The main points are that the parametrization is constrained by EM form factors, pdf’s, sum rules and some DVCS relations. A more detailed description of the other transversity functions including the first moment of  $h_1^\perp \equiv 2\tilde{H}_T^q + E_T^q$  is given in [11]. In Fig. 2 (Right) we show a small sampling of results, compared with data from Jefferson Lab, Hall B [14]. The various GPDs enter the helicity amplitudes and those, in turn, determine all the cross section terms for  $\pi^0$  electroproduction. Note that the azimuthally independent  $F_{UU,T} + \mathcal{E}F_{UU,L}$  is determined primarily by  $H_T$ , and thus provides a determination of the pdf  $h_1$  and the tensor charge  $\delta q$ . The transverse and longitudinal cross sections have been separated experimentally at small  $t$  [15]. Some preliminary data were shown and compared favorably with our predictions (see Fig.4(Right) in Ref. [20]).

DVCS observables that depend on the gluon GPDs are generally suppressed by one power of  $\alpha_s$ , since the photons connect to the gluons through quark loops. These gluon contributions will be difficult to access, being in the helicity amplitudes along with the dominant quark GPDs. The one case that directly exposes gluon contributions is through double helicity flip of the photons, which connects to the transversity gluon distributions of Eq. 2.6. To observe that effect requires precise measurements of azimuthal asymmetries, up to  $\cos 3\phi$  terms. Alternatively, electroproduction of vector mesons or lepton pairs will enable this. This phenomenology is being studied [16].

## 5. Observing GTMDs

We introduced the GTMDs above in Eq. 2.1, without reproducing the extensive decompositions into many structure functions [3]. Since these functions appear like unintegrated parton + nucleon amplitudes, they have both  $k_T$  and  $\Delta_T$ . The  $k_T$  variation arises from the patron's transverse 3-momenta relative to the nucleon average, longitudinal 3-momentum direction.  $\Delta_T$  is the momentum transfer between incoming and outgoing nucleon. As we noted in Eq. 2.1, for the GTMDs then, there are 2 planes for the kinematics, the  $k_T$  plane formed by  $\vec{k}_T, \vec{P}_3$ ; the  $\Delta$  plane formed by the  $\vec{\Delta}_T, \vec{P}_3$ . We have asked whether or not the GTMDs can be accessed experimentally. Processes that have 3 irreducible planes, like exclusive electroproduction of  $\gamma + \pi^+ + \pi^- + N$ , are candidates for indirect measurements of interesting GTMDs, particularly  $F_{14}$ , connected to orbital angular momentum [21]. In particular, we are considering

$$\gamma^*(q) + N(p) \rightarrow \pi(\vec{q}'') + \pi(\vec{q}') + \gamma^*(q') + N(p') \quad (5.1)$$

as a means to isolate the relevant GTMDs, as shown in Fig. 5.

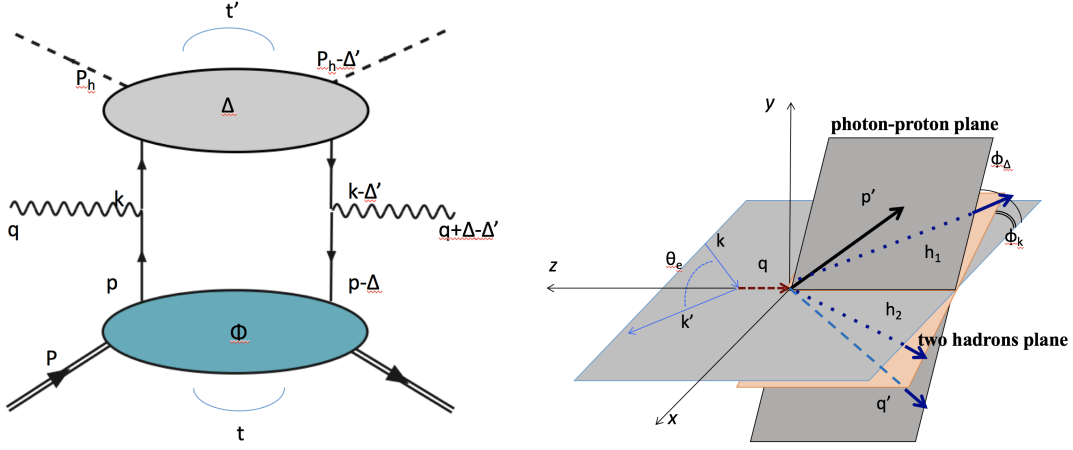


**Figure 5:** (color online) **Left:** Diagram for 3-body off-forward scattering of  $\pi, +\gamma + p$ . **Right:** Orientation of 3 planes for  $e + p \rightarrow e' + \pi^+ + \pi^- + \gamma + p'$ .

## 6. Conclusions & Outlook

We have extended all the distributions that can be accessed with our “flexible spectator” model, focusing on chiral even and odd quark GPDs, the latter entering the transversity parton distributions in the nucleon that were accessed through deeply virtual exclusive  $\pi^0$  meson production. This represents a consistent quantitative step with respect to our previous work [10]. It should be noted that, in particular,  $H_T$  and the combination  $2\tilde{H}_T + E_T$ , now are separated. A similar, somewhat simplified approach was taken also in Ref.[22] - we differ in the importance attached to the skewedness dependence of  $E_T, \tilde{E}_T$ .

We see the results of our extended approach for some of the many measured and measurable observables. What is especially gratifying is that certain asymmetries constrain the GPDs well

enough to separately determine  $H_T$ , and consequently transversity through the limit  $H_T(x, 0, 0)$ , and the combination  $2\tilde{H}_T + (1 \pm \xi)E_T$ . (See Ref. [11] for details.)

We sketched the extension of the model to the gluon distributions, which is work in progress [16] and suggested an experimental means to indirectly measure some GTMDs.

## 7. Acknowledgements

G.R.G. is grateful to the organizers of QCD-Evolution 2016 for a productive meeting. Work of S.L. supported by U.S. D.O.E. grant DE-FG02-01ER4120. We thank our collaborators, A. Courtoy, J.O. Gonzalez Hernandez, A. Rajan and J. Poage.

## References

- [1] P.J. Mulders and R.D. Tangerman, Nucl. Phys. **B 461**, 197 (1996).
- [2] D. Müller, *et al.*, Fortschr. Phys. **42**, 101 (1994); X-d. Ji, Phys. Rev. Lett. **78**, 610 (1997); A.V. Radyushkin, Phys. Lett. **B 380**, 417 (1996).
- [3] S. Meissner, A. Metz and M. Schlegel, JHEP **08**, 056 (2009).
- [4] S. Ahmad, H. Honkanen, S. Liuti *et al.*; *ibid* Eur. Phys. J. **C63**, 407-421 (2009); *ibid* Phys. Rev. **D75**, 094003 (2007).
- [5] G. R. Goldstein, J. O. Hernandez and S. Liuti, Phys. Rev. D **84**, 034007 (2011).
- [6] J. O. Gonzalez-Hernandez, S. Liuti, G. R. Goldstein and K. Kathuria, Phys. Rev. C **88**, 065206 (2013).
- [7] M. Diehl, Eur. Phys. Jour. C **19**, 485 (2001); *ibid*, Phys. Rept. **388**, 41 (2003).
- [8] X. D. Ji, Phys. Rev. D **55**, 7114 (1997)
- [9] P. Hoodbhoy and X. Ji, Phys. Rev. D **58**, 054006 (1998).
- [10] S. Ahmad, G. R. Goldstein and S. Liuti, Phys. Rev. **D79**, 054014 (2009).
- [11] G. R. Goldstein, J. .O. Gonzalez Hernandez and S. Liuti, Phys. Rev. D **91**, 114013 (2015); *ibid*, J. Phys. G: Nucl. Part. Phys. **39** (2012) 115001.
- [12] G. R. Goldstein and M. J. Moravcsik, Ann. Phys. **195**, 213 (1989).
- [13] G.D.Cates, *et al.*, Phys. Rev. Lett. **106**, 252003 (2011).
- [14] I. Bedlinskiy, *et al.*, Phys.Rev.Lett. **109**, 112001(2012).
- [15] F. Sabatie, "DVCS &  $\pi^0$  electroproduction at Hall A, Jefferson Lab", presentation at CIPANP2015, Vail, Colorado (May 2015).
- [16] J. Poage, J. O. Gonzalez-Hernandez, S. Liuti, G. R. Goldstein, work in progress.
- [17] S.I. Alekhin, Phys. Rev. **D68**, 014002 (2003).
- [18] V. Braun, P. Gornicki, L. Mankiewicz and A. Schäfer, Phys. Lett. **B 302**, 291 (1993).
- [19] J.C. Collins, L. Frankfurt, and M. Strikman, Phys. Rev. D **56**, 2982 (1997).
- [20] G. R. Goldstein and S. Liuti, PoS QCDEV2015, 051 (2015).
- [21] A. Courtoy, G. R. Goldstein, J. .O. Gonzalez Hernandez, S. Liuti, A. Rajan, Phys. Lett. **B731**, 141 (2014) ; *ibid* work in progress.
- [22] S. V. Goloskokov, P. Kroll, Eur. Phys. J. **A47**, 112 (2011).